TECHNICAL UNIVERSITY OF CLUJ-NAPOCA

ACTA TECHNICA NAPOCENSIS

Series: Applied Mathematics, Mechanics, and Engineering
Vol. 65, Issue Special III, November, 2022

IN VITRO MECHANISM WHIT PULSATIVE LASER ON THROMBOLYSIS

Dumitru Adrian DRAGHICI, Ileana PANTEA, Nadinne ROMAN, Daniela DRUGUS, Angela REPANOVICI

Abstract: *Thrombolytic therapy is the key in the treatment of acute, cardiogenic cerebral embolism caused by coagulated blood carries some risk of hemorrhagic complications, and it is necessary to develop new safer and more reliable treatment methods. Laser thrombolysis treatment, which uses as a factor the difference in energy absorption between the thrombus and the arterial wall, has shown promise as a new method of treatment, as it can act selectively, in this case only on the respective thrombus. However, it has not been applied clinically and one of the main reasons for this is that its underlying mechanism has not yet been elucidated. We have developed and analyzed a pulsed laser thrombolysis system for treating cerebral blood vessels, which consists of a diode-pumped solid-state neodymium-yttrium aluminum garnet laser, which has excellent stability and maintainability and is suitable for clinical applications coupled to a small diameter optical fiber for increased maneuverability. Moreover, we analyzed the mechanisms that occur during pulsed laser irradiation of transparent glass tubes and gelatin phantoms in various pathological cases simulated in vitro. We found that bubbles form as a thermal effect in addition to pulsed laser irradiation ablation. Additionally, we did not detect shock waves or water jets associated with generated bubbles. We carefully analyzed the dynamics and growth rate of bubbles and their effect on a rabbit blood clot phantom within them. We concluded that the bubbles generated by the laser irradiation physically cut the thrombus and therefore had a thrombectomy effect. We believe that this study will clarify the mechanism of laser thrombolysis therapy and greatly contribute to its clinical application in tomorrow's mechatronic systems.*

Key words: *laser thrombolysis, blood vessels, laser irradiation, laser treatment.*

1. INTRODUCTION

Considering the report of the Ministry of Health, cerebrovascular diseases represent one in ten deaths in the world. Acute cardiogenic cerebral embolism, in which blood flow to the brain /heart is suddenly interrupted, often causes severe, if not fatal, symptoms [1, 2]. For this reason, blood flow during cerebral embolism must be restarted as soon as possible, before the brain tissue is irreversibly damaged (within about 2.5 - 4 hours), and thrombolytic drug therapy (tissue plasminogen activator: tPA) is a first choice in the subject.

On the other hand, thrombolytic therapy increases the risk of bleeding complications, so much safer and more reliable treatment methods need to be developed [3–7]. Over time there have been rapid advances in endovascular interventional techniques, such as embolectomy with mechanical emboli removal using the Cerebral Ischemia Recovery System (Merci) (Concentric Medical, Mountain View, CA, USA) and mechanical clot aspiration with the remarkable Penumbra system (Penumbra, Alameda, CA, USA). However, endovascular interventional techniques have clinical problems, such as the risk of vascular and brain damage. Simultaneously, selective laser thrombolysis, which uses the difference in energy absorption between the thrombus and the arterial wall in the 300–600 nm wavelength band, has been attempted, and studies using a 577 nm dye laser and a 308 nm excimer laser have been tried, have been reported [8–15]. In particular,

the difference located in the range of 500 to 600 nm is expected to have a selective effect on fibrin and red blood cell-rich thrombi, which particularly cause cardiogenic cerebral embolism [10]. For example, Viator et al. reported laser thrombolysis using a pulsed laser with a wavelength of 532 nm and a pulse width of 50–200 μs [16]. They reported that irradiation generated air bubbles and suggested that the bursting of the bubbles caused a water jet effect that helped to remove the thrombus, although they did not fully clarify the underlying removal mechanism. Laser thrombolysis, like any cerebrovascular treatment, carries some risk and has not been used clinically, although many researchers have vigorously studied the effects of laser thrombolysis therapy. This may be largely since the mechanism underlying thrombus removal has not yet been fully elucidated.

1.1 Optimization of clot dissociation whit diode-pumped solid-state neodymium-yttrium

Developing a diode-pumped solid-state neodymium-yttrium aluminum garnet (Nd:YAG) laser system (wavelength: 532 nm, pulse width: 50–200 μs, repetition rate: 1–14 Hz) for clinical applications. We believe that a complete solid-state laser is suitable due to its ease of maintenance and electronic stability of the circuit. To allow irradiation of cerebral blood vessels, our system consists of a low peak power pulsed laser and an optical fiber that has a core diameter of 100 μm. Our device is easily portable and can be used in in vivo experiments. In this study reported here, clear transmission images of transparent (non-opaque) glass tubes and gelatin phantoms were obtained and a detailed analysis of the thrombus removal mechanism was attempted in an experiment on a blood clot phantom of rabbit. We found that the bubbles were generated as a thermal effect of pulsed laser irradiation. Notably, the bubble growth rate did not exceed the acoustic speed, and there was no shock wave or water jet, as had been suggested in previous reports. Therefore, we concluded that physical cutting by the bubble itself of the thrombus is removed in therapy. We believe that the results of this study will represent an important contribution to the clinical application of laser thrombolysis therapy.

2. RESEARCH METHODOLOGY

A prototype medical laser device (LA1292; Hamamatsu Photonics, Shizuoka, Japan) was developed as a pulsed laser source for laser thrombolysis with a double enclosure structure to minimize light leakage. A block diagram and a photo of the system are shown in Figure 1. This system has a diode-pumped second-harmonic Nd:YAG laser (wavelength: 532 nm). Since the laser system has a relatively large pulse width in the microsecond range, a second harmonic can be efficiently obtained by placing a potassium titanyl phosphate (KTP: KTiOPO4) crystal inside the resonator. A pulsed laser was coupled into an optical fiber through a collimating lens installed in the cabinet. To treat the thrombus in the M2 area of the middle cerebral artery (MCA) (vessel diameter ≤ 1.2mm -1 mm), a very small diameter quartz fiber (F-MCB-T; Newport Corporation, Irvine, CA, USA) was used (core diameter: 100 μm, cladding diameter: 110 μm, numerical aperture (NA): 0.22). Thus, the laser system has an average power of more than 100 mW at the tip of the fiber, with a pulse width of 50, 100 or 200 μs and a repetition rate of 1 to 14 Hz. The fiber optic connector was placed at the tip of the arm at a height sufficient to accommodate a person's movements during surgery. The connector is a non-contact type that uses an optical focusing system to prevent damage during fiber optic replacement.

Pulsed laser irradiation is controlled by a foot switch that is linked to a mechanical shutter installed in the housing, allowing the surgeon to keep both hands-free during fiber optic laser irradiation.

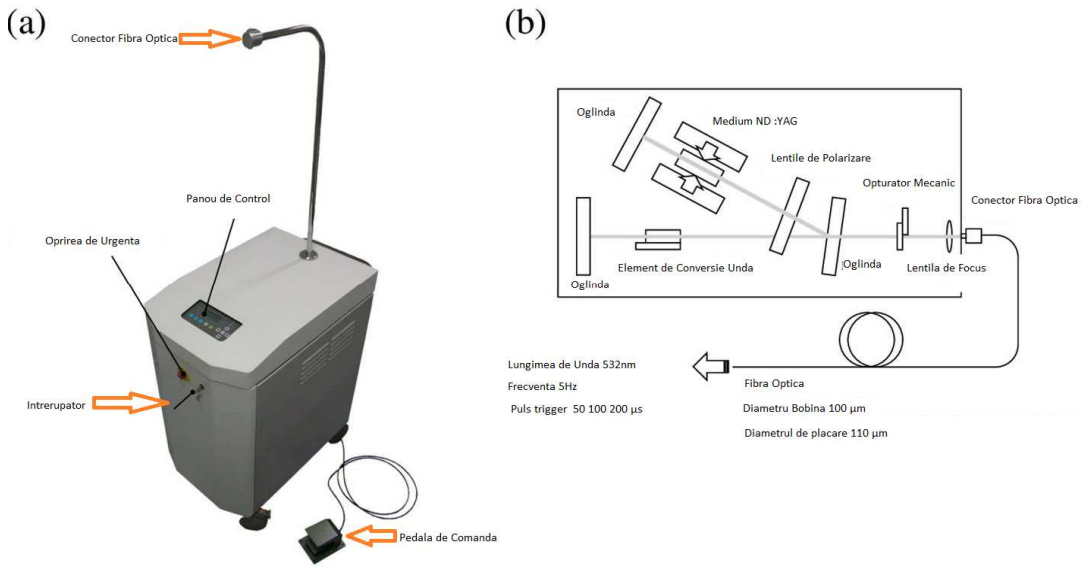

Fig. 1. Laser system: LA1292.(a) Outer view and (b) block diagram. Transportable laser irradiation system for laser thrombolysis therapy with a doddle enclosure to prevent light leakage. Width: 500 mm, Deepness: 747 mm, Height: 1 847 mm (including arm).

2.1 The research process - Laser irradiation - Dynamic analysis

The high-speed video camera (FASTCAM SAPHC; Photoron, Tokyo, Japan) was used to analyze the reaction with a single laser pulse. A block diagram of the experimental setup is shown in Figure 2. We used gelatin phantoms encapsulated in glass tubes to obtain detailed transmission images. A dye (Direct Red 81; Sigma-Aldrich, St. Louis, MO, USA) was added to 10 wt% gelatin (G2500; Sigma-Aldrich, St Louis, MO, USA) to make the absorbance of the phantom at 532 nm equal to that of blood [15, 17]. The hardness of gelatin depends on its protein concentration, but it is difficult to obtain a correlation between the mechanical strength of a gelatin phantom and that of a real thrombus [11].

Therefore, we determined the concentration of gelatin based on animal studies and experience. A glass tube with inner and outer diameters of 2 mm and 3 mm (FPT-300; Fujirika, Osaka, Japan) was filled with a 10 wt% gelatin aqueous solution, cooled until the gelatin coagulated, and then filled with saline solution. An optical fiber was inserted into the glass tube and pulsed laser irradiation was performed. The surface of the gelatin phantom was bent into a U-shape along the glass wall due to surface tension.

Therefore, the positions of the fiber tip and the gelatin phantom surface were visually judged using the camera image, and the distance between the fiber tip and the gelatin phantom surface was controlled within a 0.5 mm micrometer. The camera frame rate and exposure time were set to 2 µs/f and 10 µs, respectively. The amount of incident energy was 4–16 mJ/pulse (N = 5 in each irradiation condition). The bubble size was calculated from the measured length of the major and minor axes at the maximum size, considering the cross section of the bubble to be elliptical.

To prevent thermal dissolution of gelatin before irradiation, the room temperature during the experiment was set at 25°C. Male rabbits (10 to 12 weeks old) purchased from Japan SLC (Shizuoka, Japan) with no medical conditions were used in the analyzed study. All surgeries were performed under anesthesia by inhalation administration of isoflurane (Pfizer, New York, NY, USA) under strictly standardized conditions specified by the medical devices. All animal experiments were approved by the Hamamatsu University School of Medicine Animal Care and Use Committee (No. 2017025) in compliance with current legislation.

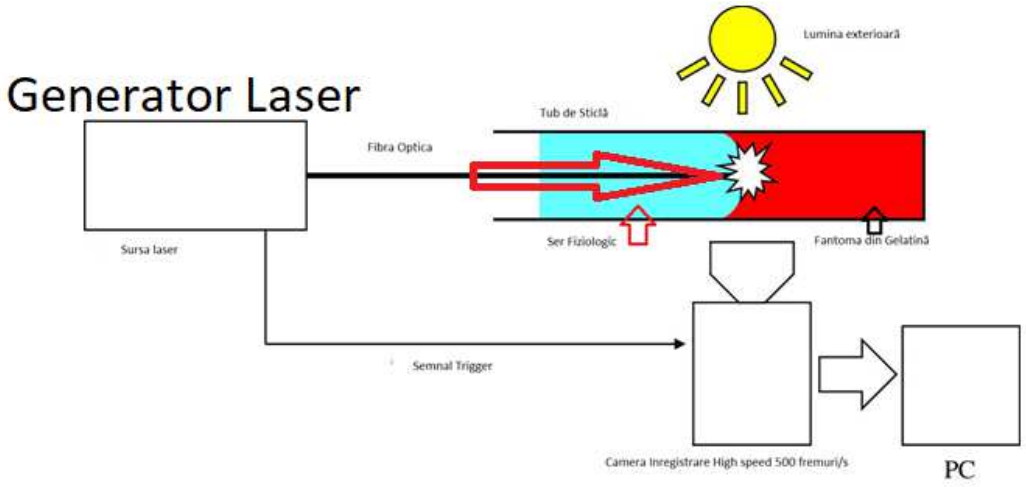

Fig. 2. Block diagram of the in vitro experiment using a high-speed camera for dynamic analysis of pulsed laser irradiation reaction. FASTCAM SAPHC; Photoron, Tokyo, Japan

The diameters of the debris generated by irradiation were evaluated using a rabbit blood clot phantom. Blood was collected directly from the carotid artery of rabbits under isoflurane anesthesia. After the blood was collected, the rabbits were sacrificed with an overdose of pentobarbital. Blood clots in a polyethylene tube were made by incubation for 40 to 50 minutes. at 37°C. As with the gelatin phantom, a glass tube with an inner diameter of 2.0 mm was filled with clot phantom along with saline. The average power was 0mW, 20mW, 40mW, 60mW, and 80mW, the pulse width was 100 μs, the frequency was 5 Hz, and the irradiation time was 10 s (0 mW: N = 3, 20–80 mW: N = 5 each) . When blood clots were continuously irradiated with a pulsed laser, the tip of the optical fiber was scorched due to coagulation of the blood cell components, she notes. The optical fiber was inserted into a polyethylene tube (inner diameter: 0.40 mm, outer diameter: 0.80 mm, KN-392-SP 28; Natsume Seisakusho, Tokyo, Japan), which resembles a type of catheter, and heparinized saline (concentration: 20 U). /mL, flow rate: 6 mL/h) was administered continuously during irradiation to prevent burning of blood clots. After irradiation, debris containing saline was collected with a silicone pipette and images of debris were taken using a phase contrast microscope (ECLIPS E200, Nikon, Tokyo, Japan) without using Giemsa staining. ImageJ image processing software was used to assess particle size.

2.2 Statistical analysis

An independent-samples t-test was used to determine significant differences in the data IBM SPSS Statistics version 26 (IBM, Armonk, NY, USA) was used.

Dynamic analysis of laser-irradiation Figure 3 showed a typical anticipated response to pulsed laser irradiation with a pulse (irradiation energy: 16 mJ/pulse, pulse width: 100 μs) in a gelatin phantom. When the laser pulse irradiated the gelatin phantom, a bubble formed at the tip of the optical fiber (Figure 3, 10 μs). The bubble (indicated by the white arrow in Figure 3) was generated within 10 μs after the start of irradiation, and the remainder of the pulse light irradiated the interior of the growing bubble.

The generated bubbles infiltrated the gelatin phantom and an ellipsoidal shape was formed which grows in the direction of irradiation. Air bubbles reached a maximum size of 2.53 mm in the long axis direction (in 2.64 ± 0.19 mm, N = 5) at 420 μs after the start of irradiation. After that, the bubbles did not burst but shrunk and disappeared, and cut marks on the gelatin phantom were found around the tip of the optical fiber at 1280 μs after the onset of irradiation.

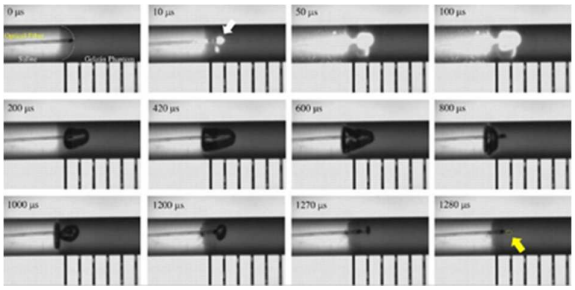

Fig. 3. Typical example of bubble generated by a pulsed laser irradiation in a gelatine ghost (incidental energy: 16 mJ/pulse, pulse width: 100 µs, frame frequency: 10 µs/f, exposure time: 2 µs) [5].

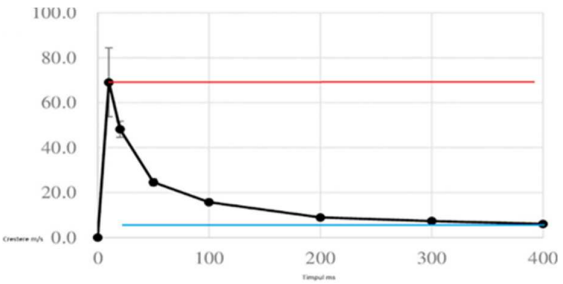

Fig. 4. The rate of growth of bubbles generated by laser irradiation in the gelatin ghost.

The maximum dimension along the short axis direction was 1.35 mm (mean: 1.42 ± 0.10 mm). After the bubble disappeared by pulsed laser irradiation and cut marks were observed in the gelatin phantom, the bubbles reappeared several times to the elasticity of the gelatin phantom.

Bubble generation, expansion, contraction, disappearance, and reappearance stopped completely after about 3300 µs (see Movie S1). The bubble growth rate showed a maximum value of 69.1 ± 15.3 m/s (N = 5) at 10µs after the onset of irradiation (Figure 4).

3. RESULTS

The dynamic analysis of laser irradiation is found in Figure 3, this shows a typical reaction to laser irradiation with a pulse (irradiation energy: 16 mJ/pulse, pulse width: 100 µs) in a ghost of gelatin. When the laser pulse irradiated the gelatin ghost, a bubble formed at the tip of the optical fiber (Figure 3, 10 µs). The bubble (indicated by the white arrow in Figure 3) was generated within 10 µs after the irradiation began, and the rest of the pulse light irradiated the inside of the growing bubble.

The bubbles generated were infiltrated into the gelatin ghost and an ellipsoidal form was formed that grows in the direction of irradiation. Bubbles reached a maximum size of 2.53 mm in the long axis direction (average 2,64 ± 0.19 mm, N = 5) at 420 µs after irradiation began. After that, the bubbles did not burst, but shrunk and disappeared, and around the tip of the optical fiber were found signs of pruning on the gelatin ghost 1280 µs after the onset of irradiation.

The maximum dimension in the direction of the short axis was 1.35 mm (average: 1.42 ± 0.10 mm). After the bubble disappeared by pulsed laser irradiation and traces of cutting in the gelatin ghost were observed, the bubbles reappeared several times due to the elasticity of the gelatin ghost. This bubble generation, expansion, contraction, extinction and recurrence completely stopped after about 3300 µs (see film S1).

The growth rate of the bubble showed a maximum value of 69.1 ± 15.3 m/s (N = 5) at 10µs after the onset of irradiation (Figure 4, horizontal axis: Time elapsed after pulse laser irradiation. Vertical axis: the rate of growth of the bubble in the direction of the long axis. The growth rate of bubbles reached a maximum of 69.1 ± 15.3 m/s (N = 5) at 10 µs after the start of irradiation.).

The following: pulse width = 100 µs (N = 5), ♦: pulse width = 200 µs (N = 5). Horizontal axis: incident energy per pulse. Vertical axis: the projected area of the bubble assuming it's an ellipse. In both 8, 16 mJ/puls, bubbles that were generated with a pulse width of 200 µs were significantly lower than those generated with a pulse width of 100 µs (*,**; P & L; 0.05).

Leakages of debris from the rennet ghost were observed just before pulsed laser irradiation because of continuous administration of heparinized saline solution. However, a significant generation of debris was observed only after laser irradiation (Figure 6 (A) and S2 Movie). Figure 6(B) presents a typical example of debris [9].

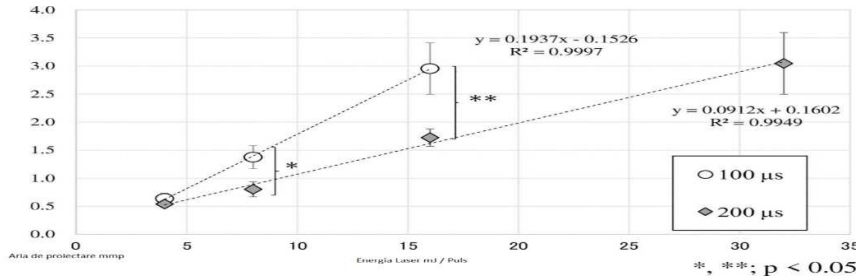

Fig. 5. The relationship between irradiation energy and bubble projection area.

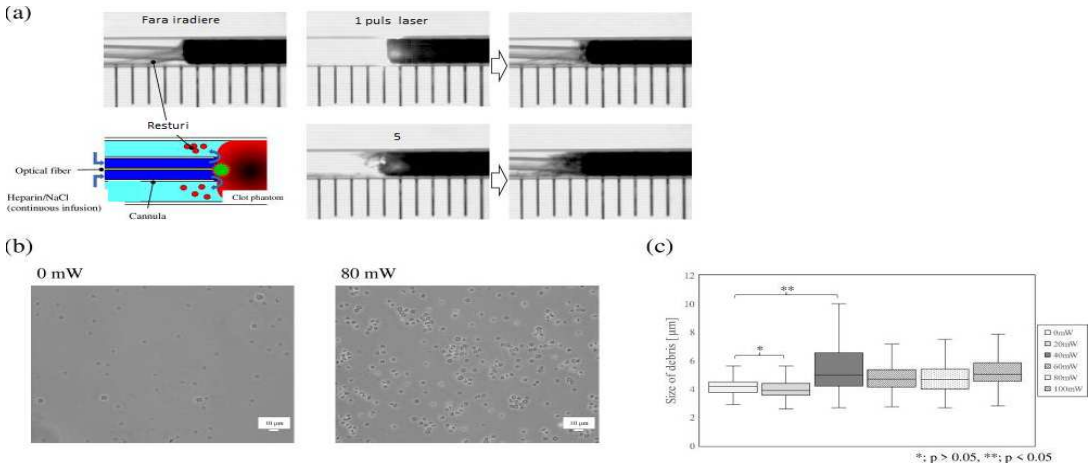

Fig. 6. The blood clot ghost was irradiated with a pulsed laser and the size of the debris generated was assessed. Assessment of the size of debris.

Rests mainly consist of single red blood cells and red blood cell aggregates [18]. The size of the largest piece of debris detected was 44 µm, but the dimensions of more than 98 % of the scrap pieces were less than 20 µm. There have been few changes in red blood cell morphology. Figure 6(C) show research results; the mean ratio of debris observed in each mean power condition from 0 to 80 mW (0 mW: N = 3, 20-80 mW: N = 5). More than 93 % of the waste sizes were less than 6 µm under irradiation conditions with an average power of not more than 20 mW. On the other hand, the number of red blood cell aggregates greater than 6 µm was significantly higher at an average power of 40 mW or more (p &l; 0.05).

Figure 6, Typical response of the clot ghost to pulsed laser irradiation. (a) Block diagram and real images of the in vitro phantom experiment. A significant generation of debris was observed after pulse irradiation. Incidence energy: 16 mJ/pulse, pulse width: 100 µs, frequency: 5 Hz, frame rate: 60 fps, exposure time: 250 µs. A glass tube (internal diameter: 2 mm) was filled with a ghost of blood clot and saline solution, and pulsed laser irradiation was carried out continuously for 10 seconds (total: 50 photos).

The optical fiber was inserted into a polyethylene tube (inner diameter: 0.40 mm, outer diameter: 0.80 mm), resembling a catheter, to prevent the burning of blood clots, and heparinized saline solution (concentration: 20 U/mL, flow rate: 6 mL/h) was administered continuously during irradiation to prevent blood clots from burning.

Superior group of photos: before irradiation and after irradiation with a pulse. Lower group of photos: after irradiation with five pulses. The boundary between the blood clot ghost and the saline solution became unclear as the number of irradiations increased. (B)Results collected after 10 s of irradiation and observed under a phase contrast microscope (no staining). The average power was 0 mW (left) and 80 mW (right). (C) The size of the debris (*; P > 0,05, **; P & L; 0,05, Vertical axis: the size of the debris observed after irradiation). Ratio of aggregates generated in each laser irradiation condition.

Results of irradiation of rabbit blood clot ghost. Pulse width: 100 µs. Rehearsal: 5 Hz.

Debris less than 6 μm were unique red blood cells. The percentage of aggregated red blood cells above 6 μm was recorded for each size.

It has been suggested that laser thrombolysis during pulse laser irradiation involves cutting by generated bubbles and generating water jets, as well as laser ablation, [16] and the dynamic analysis in our study showed that bubbles formed after laser irradiation. Bubbles were generated within 10 μs after the onset of pulsed laser irradiation (Figure 3). The pulse width was 100 μs and it was estimated that 1.6 mJ (10 % of the total incident energy of 16 mJ) contributed to bubble generation. Absorbance A [log10] of blood (hemoglobin 4 hem, HbO2: 43.876 [cm-1/M], Hb: 40,584 [cm-1/M]) at 532 nm for a cell is 0,93. Assuming that 0.1 mm from the tip of the optical fiber is filled with blood, the absorbance is A′ = 93.0×0.01 1 and there is no scattering in the gelatin ghost, the volume of pulsed laser V is defined as a cone throne according to the NA of the optical fiber.

Since the concentration of the gelatin ghost is 10 % by weight, which can be assumed to be close to water, the amount of heat needed to raise a quantity of water corresponding to the volume of the irradiation area from 25 to the boiling point (100 %). it's about 0.25 mJ. After the bubbles were formed, the pulsed laser irradiated the inside of the growing bubbles. Since the thermal insulation time in the gelatin ghost is estimated at 35 ms [16], it was assumed that pulses between 10 and 100 μs also had a thermal effect. However, no bubbles between 10 and 100 μs were generated after the first bubble was generated.

In the case of pulse laser irradiation with the same incident energy, bubbles generated under irradiation conditions with a pulse width of 100 μs were greater than bubbles generated under irradiation conditions with a pulse width of 200 μs (Figure 5). That is, the peak power of the pulsed laser affected the generation and growth of bubbles. There has been used an optical fiber with a core diameter of 100 μm. When a single laser pulse irradiated with an average power of 80 mW (pulse width: 100 μs), we can calculate that the power density at the top of the fiber was 2.1 MW/cm². At 1 mm from the tip of the fibre, the size of the spot was approximately 0.5 mm (NA fiber: 0.22) and the power density was 81.5 W/cm².

Moreover, the power density at an average power of 20 mW was 4.1 W/cm², suggesting that ablation occurred in the irradiated area of the ghost of gelatin and blood clot due to the small size of the optical fiber irradiation point [15]. At the same time, Viator et al. reported that the effect of ablation was limited [16].

In this study, we used glass tubes and transparent gelatin ghosts to perform a dynamic analysis of pulsed laser irradiation using detailed transmission images. We observed bubble dynamics and bubble removal effect on the thrombus immediately after laser irradiation. We found that the bubbles contracted and disappeared without breaking out. The observed bubbles formed all elliptical forms that increased in the direction of irradiation.

The growth rate of the bubbles was 69.1 ± 15.3 m/s (N = 5), which was much lower than the speed of sound in water. T. Hirano et al. reported removal of thrombus by Ariete hammer effect of laser-induced liquid jet without shock wave generation [19, 20]. In our experiment, the distance between the tip of the optical fiber and the ghost surface was set at 0.5 mm. Therefore, depending on the irradiation conditions, the water may have penetrated between the tip of the optical fiber and the surface of the ghost and have been pushed by bubbles.

However, the structure of the coating is important for generating and controlling water jets. In our study, although some directionality was observed in the direction of bubble growth, most bubbles increased as infiltration into the ghost, and the effect of the jet of water, which may or may not have occurred, was considered to be limited. It has also been reported that the repetitive mechanical action of water jets or an ultrasound induced cavitation mechanism can cause thrombus fragmentation and increase the contact area of a fibrinolytic agent [21].

As shown in Figure 4, bubbles were generated even under irradiation conditions with an average power of 20 mW. And more than 93 % of the debris was red blood cells. Accordingly, the percentage of erythrocyte aggregates in debris has been significantly increased under irradiation conditions with an

average power of 40 mW or more. The amount of incident energy correlates with the size of the bubbles generated, and our experimental results have suggested that the deformation of thrombus due to bubble generation is an important factor in the thrombus removal effect. The blood clot ghost used in this study was whole blood clotted with fibrin clot, which may partially reflect the structure of red blood clots targeted by laser thrombolysis therapy [22, 23].

As shown in Figure 6 (B), phase contrast microscopic images of the debris generated by laser irradiation showed that red blood cells existed as individual cells or discrete aggregates. In addition, there have been few changes in the morphology of red blood cells. That is, the generation of debris, which were aggregated by red blood cells, indicates that the deformation of the thrombus ghost through air bubbles cuts the fragile part of the fibrin network. Fibrin networks are known to be fibrin glues used in surgery and other applications and have been reported to have some mechanical strength [24]. Although ablation occurred even at an average power of 20 mW, the result that erythrocytic aggregates did not significantly increase unless the average power was 40 mW or higher may indicate the existence of a threshold for physical action (Figure 6(C)). Of course, it is believed that when bubbles are generated in a blood vessel rather than in a glass tube, the wall of the vessel can be deformed by the pressure generated by the bubbles.

The bubbles did not reach the walls of the glass tube in this study, so the effect of the hardness of the glass material is expected to have been small [9, 17]. The glass tube phantom model does not completely recreate an in vivo vascular situation. The absolute value of the actual duration of the in vivo bubble is considered to be variable. Similarly, it is very difficult to obtain a correlation between the mechanical resistance of the ghost and the thrombus [11]. This is because the mechanical properties of the thrombus formed in vivo are affected by various factors, such as the passage of time and individual differences. Thus, in this paper, the mechanism of laser thrombolysis was elucidated by using glass tubes and transparent gelatin ghosts to obtain detailed transmission images, but the amount of cutting was not examined. These problems need to be addressed by building more detailed in vitro models in the future. We believe that the debris generated by laser irradiation will be released into the bloodstream and become smaller aggregates or unique red blood cells through the fibrinolytic effect in vivo, like what happens with small fragments generated by the thrombolytic agents acting enzymatically on the fibrin networks. Moreover, we found that the bubbles infiltrate into the thrombus. This suggests that bubbles could be used in combination with a thrombolytic agent acting on the thrombus surface to enhance their mutual effects on a larger volume of thrombus.

4. CONCLUSIONS

To accurately determine the detailed mechanism of laser thrombolysis, a detailed physical-dynamic analysis of bubbles generated by pulsed laser irradiation was performed using transparent gelatin phantoms and clot phantoms. Our results found that in laser thrombolysis, the thrombus could be removed by breaking down the air bubbles generated by the laser irradiation.

In the future, we will analyze the reaction mechanism in more detail, including the evaluation of the amount of cutting, to determine optimal and safe irradiation conditions for the surrounding tissue. In addition, we will further investigate laser thrombolysis by performing the in vivo experiment to obtain optimal irradiation conditions necessary for the treatment, and we will research and develop new peripheral technologies that can increase the survival rate in certain clinical pathologies.

5. REFERENCES

[1] Adibhatla, R.M., Hatcher, J.F. *Tissue plasminogen activator (tPA) and matrix metalloproteinases in the pathogenesis of stroke: therapeutic strategies*, CNS Neurol Disord-Drug Targets Former Curr Drug Targets-CNS Neurol Disord, 7, pp. 243–253, 2008.

[2] Jauch, E.C., Saver, J.L., Adams, H.P. Jr, Bruno, A., Connors, J.J., Demaerschalk, B.M., et al. *Guidelines for the early management of patients with acute ischemic stroke: a guideline for healthcare professionals from the American Heart Association*, American Stroke Association, 44, pp. 870–947, 2013.

[3]. Disorders NI of N, Group Srt-PSS. *Tissue plasminogen activator for acute ischemic stroke*, N Engl J Med., 333, pp.1581–1588, 1995.

[4]. Hacke, W., Brott, T.G., Caplan, L., Meier, D., Fieschi, C., Von Kummer, R., et al. *Thrombolysis in acute ischemic stroke: Controlled trials and clinical experience*, Neurology, 53 (7 SUPPL. 4), pp. S3–S14, 1999.

[5] Manning, N.W., Campbell, B.C., Oxley, T.J., Chapot, R. *Acute ischemic stroke: time, penumbra, and reperfusion*, Stroke; 45, pp. 640–644, 2014.

[6] Wardlaw, J.M., Sandercock, P.A.G., Berge, E. *Thrombolytic therapy with recombinant tissue plasminogen activator for acute ischemic stroke: where do we go from here? A cumulative meta-analysis*, Stroke, 34, pp. 1437–1442, 2003.

[7] Lo, E.H., Broderick, J.P., Moskowitz, M.A. *tPA and proteolysis in the neurovascular unit*, Stroke, 35, pp.354–356, 2004.

[8] Shangguan, H., Casperson, L.W., Prahl, S.A. *Microsecond laser ablation of thrombus and gelatin under clear liquids: Contact versus noncontact*, IEEE J Sel Top Quantum Electron, 2, pp. 818–825, 1996.

[9] Sathyam, U.S., Shearin, A., Prahl, S.A. *Visualization of microsecond laser ablation of porcine clot and gelatin under a clear liquid*, Proceedings of Lasers in Surgery: Advanced Characterization, Therapeutics, and Systems VI. PHOTONICS WEST '96, 1996 Jan 27-Feb 2; San Jose, CA, United States: SPIE; 1996.

[10] Sathyam, U.S., Shearin A., Chasteney, E.A., Prahl, S.A. *Threshold and ablation efficiency studies of microsecond ablation of gelatin under water*, Lasers Surg Med Off J Am Soc Laser Med Surg.,19, pp. 397–406, 1996.

[11] Janis, A.D., Buckley, L.A., Nyara, A.N., Prahl, S.A., Gregory, K. *A reconstituted in vitro clot model for evaluating laser thrombolysis*, J. Thromb Thrombolysis, 13, pp. 167–175, 2002.

[12] Godwin, R.P., Chapyak, E.J., Prahl, S.A., Shangguan, H. *Laser mass-ablation efficiency measurements indicate bubble-driven dynamics dominate laser thrombolysis*, Proceedings of Lasers in Surgery: Advanced Characterization, Therapeutics, and Systems VIII. BIOS '98 INTERNATIONAL BIOMEDICAL OPTICS SYMPOSIUM 1998 Jan 27–29; San Jose, CA, United States, SPIE, 1998.

[13] Shangguan, H., Casperson, L.W., Gregory, K.W., Prahl, S.A. *Penetration of fluorescent particles in gelatin during laser thrombolysis*, Proceedings of Lasers in Surgery: Advanced Characterization, Therapeutics, and Systems VII. BIOS '97, PART OF PHOTONICS WEST 1997 Feb 8–14; San Jose, CA, United States, SPIE; 1997.

[14] Janis, A.D., Buckley, L.A., Gregory, K.W. *Laser thrombolysis in an in-vitro model*, Proceedings of Lasers in Surgery: Advanced Characterization, Therapeutics, and Systems X. BIOS 2000 THE INTERNATIONAL SYMPOSIUM ON BIOMEDICAL OPTICS 2000 Jan 22–28; San Jose, CA, United States, SPIE; 2000.

[15] Viator, J.A., Prahl, S.A. *Laser thrombolysis using a millisecond frequency-doubled Nd-YAG laser*, Proceedings of Laser-Tissue Interaction IX. BIOS '98 INTERNATIONAL BIOMEDICAL OPTICS SYMPOSIUM 1998 Jan 27–29; San Jose, CA, United States, SPIE; 1998.

[16] Viator, J.A., Prahl, S.A. *Laser thrombolysis using long pulse frequency-doubled Nd: YAG lasers*. Lasers Surg Med Off J Am Soc Laser Med Surg., 25, pp. 379–388, 1999.

[17] Casperson, L.W., Shangguan, H,. Paisley, D.L., Prahl, S.A. *Photographic studies of laser-induced bubble formation in absorbing liquids and on submerged targets: implications for drug delivery with microsecond laser pulses*, Opt Eng., 37(8), pp. 2217–2226, 1998.

[18] Suckow, M.A., Stevens, K.A., Wilson, R.P. *The laboratory rabbit, guinea pig, hamster, and other rodents*, Academic Press, 2012.
[19] Nakagawa, A., Hirano, T., Komatsu, M., Sato, M., Uenohara, H., Ohyama, H., et al. *Holmium: YAG laser-induced liquid jet knife: Possible novel method for dissection*, Lasers Surg Med., 31, pp. 129–135, 2002.
[20] Hirano, T., Nakagawa, A., Ohki, T., Uenohara, H., Takayama, K., Tominaga, T. *A laser-induced liquid jet catheter system: a novel endovascular device for rapid and reliable fibrinolysis in acute cerebral embolism*, Min-Minim Invasive Neurosurg., 51, pp. 324–328, 2008.
[21] Alexandrov, A.V., Molina, C.A., Grotta, J.C., Garami, Z., Ford, S.R., Alvarez-Sabin, J., et al. *Ultrasound-enhanced systemic thrombolysis for acute ischemic stroke*, N Engl J Med. 351, pp. 2170–2178, 2004.
[22] Wolberg, A.S., Aleman, M.M., Leiderman, K., Machlus, K.R. *Procoagulant Activity in Hemostasis and Thrombosis: Virchow's Triad Revisited*, Anesth Analg. 114, pp. 275–285, 2012.
[23] Versteeg, H.H., Heemskerk, J.W.M., Levi, M., Reitsma, P.H. *New Fundamentals in Hemostasis*, Physiol Rev., 93, pp. 327–358, 2013.
[24] Naganuma, M., Akiyama, M., Takaya, H., Sakuma, K., Kumagai, K., Kawamoto, S., et al. *Maximization of the sealing effect of fibrin glue in aortic surgery*, Gen Thorac Cardiovasc Surg., 68, pp. 18–23, 2020.

Mecanism in vitro cu laser pulsativ în tromboliză

Rezumat: Terapia trombolitică este cheia în tratamentul emboliei cerebrale acute, cardiogene, cauzate de sângele coagulat, Terapia prezintă un anumit risc de complicații hemoragice și este necesară dezvoltarea unor noi metode de tratament mai sigure și mai fiabile. Tratamentul trombolizei laser, care folosește ca factor diferența de absorbție a energiei dintre tromb și peretele arterial, s-a arătat promițătoare ca metodă nouă de tratament, întrucât poate acționa selectiv, doar asupra trombului respectiv. Cu toate acestea, nu a fost aplicat clinic și unul dintre principalele motive pentru aceasta este că mecanismul său de bază nu a fost încă elucidat. S-a dezvoltat și analizat un sistem de tromboliză cu laser pulsat pentru tratarea vaselor de sânge cerebrale, care constă dintr-un laser granat din neodim-itriu aluminiu în stare solidă pompat cu diodă, care are stabilitate și menținere excelente și este potrivit pentru aplicații clinice cuplate la un diametru mic. Mai mult, s-au analizat mecanismele care apar în timpul iradierii laser pulsate a tuburilor de sticlă transparente și a fantomelor de gelatină în diferite cazuri patologice simulate in vitro. S-a descoperit că bulele se formează ca efect termic pe lângă ablația cu iradiere cu laser pulsat. În plus, nu am detectat unde de șoc sau jeturi de apă asociate cu bulele generate. S-a analizat dinamica și rata de creștere a bulelor și efectul lor asupra unei fantome de cheag de sânge de iepure din ele. Am ajuns la concluzia că bulele generate de iradierea laser au tăiat fizic trombul și, prin urmare, au avut un efect de trombectomie. Acest studiu va clarifica mecanismul terapiei cu trombolizei laser și va contribui foarte mult la aplicarea sa clinică în sistemele mecatronice de mâine

Dumitru Adrian DRĂGHICI, PhD student, Transilvania University of Braşov, Faculty of Product Design and Environment, Braşov, România, draghicidumitruadrian@yahoo.com, 29 Bulevardul Eroilor, Brașov 500036, Romania.
Ileana PANTEA, Professor, PhD, Transilvania University of Braşov, Faculty of Medicine, Brasov, Romania, ileana.pantea@unitbv.ro, 29 Bulevardul Eroilor, Brașov 500036, Romania.
Nadinne ROMAN, Professor, PhD, Transilvania University of Braşov, Faculty of Medicine, Brasov, Romania, nadinneroman@unitbv.ro, 29 Bulevardul Eroilor, Brașov 500036, Romania.
Daniela DRUGUȘ, Professor, PhD, Gr. T. Popa Medicine University, Iasi, Romania, daniela.drugus@umfiasi.ro.
Angela REPANOVICI, Professor, PhD. Eng., PhD Marketing, Transilvania University of Braşov, Faculty of Product Design and Environment, arepanovici@unitbv.ro, 29 Bulevardul Eroilor, Brașov 500036, Romania.